Analysis of image gathers in factorized VTI media

Debashish Sarkar and Ilya Tsvankin
Center for Wave Phenomena, Colorado School of Mines

ABSTRACT

Image gathers generated after prestack depth migration are sensitive to the velocity field and are often used in migration velocity analysis for isotropic media. Here, we present an analytic and numerical study of P-wave image gathers in transversely isotropic media with a vertical symmetry axis (VTI) and establish the conditions for flattening the gathers and positioning them at the true reflector depth. Application of the weak-anisotropy approximation leads to concise expressions for image gathers of horizontal events in homogeneous and factorized $v(z)$ media in terms of the VTI parameters and the vertical velocity gradient k_z. Flattening image gathers for any reflector dip requires accurate values of the zero-dip NMO velocity at the surface ($V_{\rm nmo}$), the gradient k_z, and the anellipticity coefficient η. For a fixed error in $V_{\rm nmo}$ and k_z, the magnitude of residual moveout on image gathers decreases with dip, while the moveout caused by an error in η reaches its maximum for intermediate (under 90°) dips. Flat image gathers in VTI media, however, do not guarantee the correct depth scale of the model because reflector depth depends on the vertical migration velocity.

For factorized $v(x,z)$ media with a linear velocity variation in the x- and z-directions, the moveout on image gathers is controlled by four parameter combinations: $V_{\rm nmo}$ (x=z=0), k_z, η, and a combination of the horizontal velocity gradient k_x and the Thomsen parameter δ ($k_x\sqrt{1+2\delta}$). If too high a value of any of these four quantities is used in migration, the image gathers curve down (i.e., depth increases with offset) while a negative error causes the opposite sign of residual moveout. Lateral heterogeneity tends to increase the sensitivity of image gathers to the parameter η, and errors in η lead to measurable residual moveout of horizontal events in $v(x,z)$ media even for offset-to-depth ratios close to unity.

These results provide a basis for extending to VTI media conventional velocity-analysis methods operating with image gathers. Although P-wave traveltimes alone cannot be used to separate anisotropy from lateral heterogeneity (i.e., k_x is coupled to δ), moveout on image gathers constrains the vertical gradient k_z. Hence, it may be possible to build VTI velocity models in depth by supplementing reflection data with minimal *a priori* information, such as the vertical velocity at the top of the factorized VTI layer.

Key words: image gathers, vertical transverse isotropy, factorized media, P-waves

Introduction

The offset-depth gather (often called the "image gather") is obtained after prestack depth migration by representing migrated depth (z) as a function of half-offset (h). If the velocity model is correct, a reflection event is migrated to the same depth for all source-receiver pairs, and the corresponding image gather is flat [$z(h)$ = const].

Errors in the velocity model may cause the migrated depth to be dependent on offset, which results in residual moveout on the image gathers. Due to their high sensitivity to the velocity field, image gathers provide both a simple visual check and a valuable quantitative diagnostic tool for migration velocity analysis. Note, however, that velocity estimation using image gathers (as well as any other technique) typically requires *a priori* information to reduce the nonuniqueness inherent in thisi inverse problem.

Existing work on the application of image gathers in velocity analysis is largely restricted to isotropic subsurface models (e.g., Al-Yahya, 1987; Stork, 1991; Liu, 1995; Meng, 1999; Zhu et. al., 1998; Brandsberg-Dahl, 2001). For example, Liu (1995) developed an analytic approach for inverting the residual moveout on image gathers and computing corrections (updates) of the velocity model. However, ubiquitous evidence for the strong influence of seismic anisotropy on reflection moveout (e.g., Thomsen, 1986; Alkhalifah, 1996; Tsvankin, 2001) suggests that flattening of image gathers using purely isotropic models can often lead to erroneous velocity fields and distortions in migrated sections.

Common problems caused by ignoring anisotropy in seismic imaging include mis-ties in time-to-depth conversion, the loss of dipping energy during dip-moveout (DMO) correction, and mispositioning of migrated dipping events (e.g., Banik, 1984; Alkhalifah et al., 1996; Tsvankin, 2001). Jaramillo and Larner (1995) studied anisotropy-induced errors in prestack depth migration and showed that isotropic migration algorithms cannot flatten image gathers for a wide range of transversely isotropic (TI) models. Recent field-data observations by Peng and Steenson (2001) of image gathers with "hockey-stick" patterns (i.e., with residual moveout) that cannot be removed by conventional isotropic methods corroborate Jaramillo and Larner's (1995) conclusions.

Here, we analyze P-wave image gathers for the most common anisotropic model – transverse isotropy with a vertical symmetry axis (VTI media). In contrast to a single scalar velocity responsible for isotropic P-wave propagation, the kinematic signatures of P-waves in VTI media are governed by three parameters: the vertical velocity V_{P0} and Thomsen's (1986) anisotropic coefficients ϵ and δ (Tsvankin and Thomsen, 1994; Tsvankin, 2001). The goal of this work is to study the residual moveout on image gathers caused by errors in these parameters and to establish the conditions needed to flatten and correctly position image gathers in homogeneous and factorized [$v(z)$ and $v(x,z)$] VTI media.

The function $z(h)$ that defines an image gather is obtained by solving the following set of equations:

$$\begin{aligned} \tau_s(\boldsymbol{x_s}, x, z) + \tau_r(x, z, \boldsymbol{x_r}) &= t(y,h)\,, \\ \frac{\partial \tau_s}{\partial y} + \frac{\partial \tau_r}{\partial y} &= \frac{\partial t}{\partial y}\,, \end{aligned} \qquad (1)$$

where y is the common midpoint, τ_s is the traveltime from the source ($\boldsymbol{x_s}$) to the reflection point (x,z) and τ_r is the traveltime from the receiver ($\boldsymbol{x_r}$) to the point (x,z). Equation (1) suggests that image gathers depend solely on the traveltimes from the reflection point to the source and receiver, which implies that flattening an image gather is equivalent to accurately fitting the corresponding reflection traveltimes. However, image gathers are generated in the depth domain and carry information about the dependence of migrated depth on the anisotropic parameters and offset. Therefore, distortions of image gathers computed for an inaccurate anisotropic model require a separate analysis that cannot be performed on reflection-moveout curves.

Generally, equation (1) does not lend itself to closed-form expressions, even for isotropic media (Liu, 1995). Analytic treatment of image gathers is much more involved in anisotropic media because of the velocity variation with propagation angle and the increased number of the medium parameters. Hence, most analytic solutions in this paper are based on the weak-anisotropy approximation linearized with respect to the parameters ϵ and δ. The linearized equations, which reveal the influence of the VTI parameters on image gathers, are verified by performing numerical tests for a representative set of VTI models.

Algorithms for modeling and prestack depth migration

The first step in the numerical analysis of image gathers was to generate synthetic seismograms of P-wave reflections in homogeneous or factorized VTI media using SU (Seismic Unix) code *susynlvfti*. To build the traveltime tables for prestack depth migration, we employed the anisotropic ray-tracing algorithm of Alkhalifah (1995). The traveltimes τ computed along each ray were then extrapolated to adjacent grid points using the paraxial approximation described by Gajewski and Pšenčík (1987):

$$\begin{aligned} \tau(\mathbf{x}) = \tau(\bar{\mathbf{x}}) + p_k(\bar{\mathbf{x}}).(x_k - \bar{x}_k) \\ + \frac{1}{2} N_{ik}(\bar{\mathbf{x}}).(x_i - \bar{x}_i).(x_k - \bar{x}_k)\,, \end{aligned} \qquad (2)$$

where $\mathbf{x}$ corresponds to the point where we seek to find the traveltime, $\bar{\mathbf{x}}$ defines the coordinate of the point on the central ray from which the traveltime is extrapolated, $\mathbf{p}$ is the slowness vector [$p_k(\bar{\mathbf{x}}) = \frac{\partial \tau}{\partial x_k}\Big|_{\bar{\mathbf{x}}}$], and $N_{ik}(\bar{\mathbf{x}}) =$

$\frac{\partial^2 \tau}{\partial x_k \partial x_i}\Big|_{\bar{\mathbf{x}}}$. Following Gajewski and Pšenčík (1987), the matrix of the second traveltime derivatives N_{ik} can be written as

$$N_{ik} = \frac{\partial p_i}{\partial x_k} = \frac{\partial p_i}{\partial \gamma_j}\left(\frac{\partial x_k}{\partial \gamma_j}\right)^{-1}, \qquad (3)$$

where γ_1 is the takeoff angle at the source (usually denoted by ψ) and $\gamma_2 = \tau$. The slownesses $p_k(\bar{\mathbf{x}})$ and the derivatives $\frac{\partial p_i}{\partial \tau}$ and $\frac{\partial x_k}{\partial \tau}$ can be computed while tracing the central ray.

However, the derivatives $\frac{\partial p_i}{\partial \psi}$ and $\frac{\partial x_k}{\partial \psi}$ are evaluated along the wavefront [for a constant τ], which requires tracing at least one additional (auxiliary) ray. If $\psi+\Delta\psi$ is the takeoff angle of an auxiliary ray, then the derivatives with respect to ψ can be found by linear interpolation for a fixed traveltime τ:

$$\frac{\partial p_i}{\partial \psi} \approx \frac{p_i(\psi+\Delta\psi) - p_i(\psi)}{\Delta\psi},$$
$$\frac{\partial x_i}{\partial \psi} \approx \frac{x_i(\psi+\Delta\psi) - x_i(\psi)}{\Delta\psi}. \qquad (4)$$

The extrapolated traveltimes $\tau(\mathbf{x})$ were estimated by evaluating equations (3) and (4) to compute N_{ik}, and then substituting N_{ik} into equation (2). The anisotropic ray-tracing algorithm and the time-extrapolation procedure are incorporated in the new SU code *rayt2dan*. The traveltime tables were used in a Kirchhoff prestack depth migration code originally designed for isotropic models (*sukdmig2d*, written by Liu, 1995) to generate image gathers in VTI media.

Homogeneous VTI media

Due to the difficulty in solving equation (1) for VTI media, the function $z(h)$ describing an image gather is obtained in Appendix A using the weak-anisotropy approximation. For a horizontal reflector embedded in a homogeneous VTI medium, linearization in the parameters ϵ and δ yields

$$z_M^2(h) = \gamma^2 z_T^2 - h^2 V_{P0,M}^2 \left(\frac{1}{V_{\mathrm{nmo},M}^2} - \frac{1}{V_{\mathrm{nmo},T}^2}\right) + 2\,\frac{h^4}{h^2+z_T^2}\left(\eta_M \frac{V_{\mathrm{nmo},M}^2}{V_{\mathrm{nmo},T}^2} - \eta_T \frac{V_{\mathrm{nmo},T}^2}{V_{\mathrm{nmo},M}^2}\right), \qquad (5)$$

where the subscript T refers to the true model and M to the model used for migration, $z_M(h)$ is the migrated depth for the half-offset h, z_T is the true depth of the zero-offset reflection point, $\gamma \equiv V_{P0,M}/V_{P0,T}$ is the ratio of migration and true vertical velocities, $V_{\mathrm{nmo}} = V_{P0}\sqrt{1+2\delta}$ is the zero-dip normal-moveout (NMO) velocity, and $\eta \equiv (\epsilon-\delta)/(1+2\delta)$ is the Alkhalifah–Tsvankin (1995) anellipticity parameter responsible for time processing of P-wave data in VTI media.

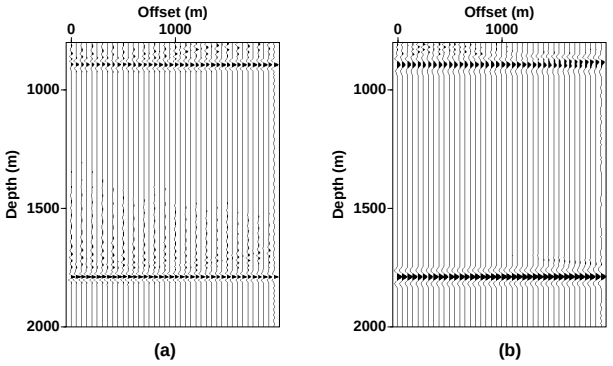

Figure 1. Image gathers for (a) two horizontal reflectors and (b) two reflectors dipping at 30° embedded in a homogeneous VTI medium. The model parameters are $V_{P0,T} = 2000$ m/s, $\epsilon_T = 0.1$, and $\delta_T = -0.1$. Prestack depth migration was performed for a different model that has the correct $V_{\mathrm{nmo},M} = V_{\mathrm{nmo},T} = 1789$ m/s and $\eta_M = \eta_T = 0.25$ ($V_{P0,M} = 1789$ m/s, $\epsilon_M = 0.25$, and $\delta_M = 0$). In the true model, the maximum offset-to-depth ratio $x_{\max}/z = 2h_{\max}/z$ is equal to two for the shallow reflector and one for the deep reflector.

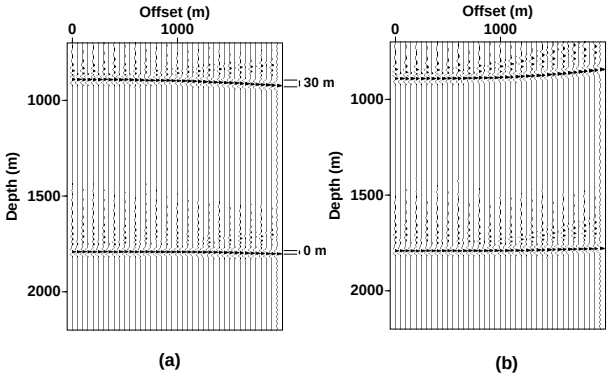

Figure 2. Image gathers for two horizontal reflectors computed for inaccurate values of η. The true model parameters and maximum offsets are the same as in Figure 1. Migration was done with $V_{\mathrm{nmo},M} = V_{\mathrm{nmo},T}$ and (a) $\eta_M - \eta_T = 0.15$ ($V_{P0,M} = 1789$ m/s, $\epsilon_M = 0.4$, and $\delta_M = 0$); (b) $\eta_M - \eta_T = -0.15$ ($V_{P0,M} = 1789$ m/s, $\epsilon_M = 0.1$, and $\delta_M = 0$).

Equation (5) shows that the moveout of horizontal events on an image gather is fully controlled by the parameters V_{nmo} and η. If the migration and true values are identical ($V_{\mathrm{nmo},M} = V_{\mathrm{nmo},T}$ and $\eta_M = \eta_T$), the migrated depth $z_M(h)$ [equation (5)] is independent of the offset h, and the image gather is flat. Although equation (5) was derived for a horizontal reflector, the correct values of V_{nmo} and η are sufficient for removing residual moveout on image gathers of dipping events as well (see the numerical examples below). This conclusion follows from the general result of Alkhalifah and Tsvankin (1995) who proved that P-wave reflection moveout in VTI media with a laterally homogeneous overburden depends only

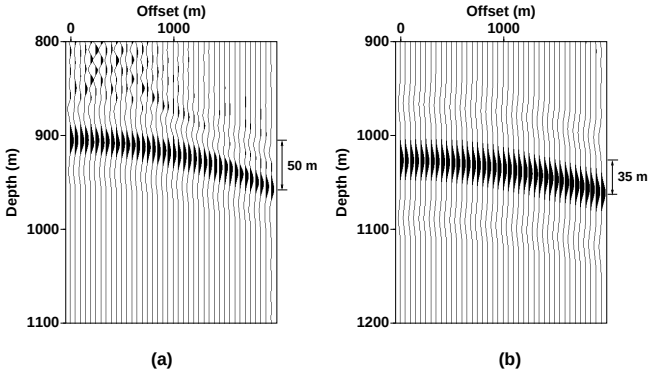

Figure 3. Image gathers for reflectors dipping at (a) 30° and (b) 45° computed for an overstated value of η. The true parameters are $V_{\mathrm{nmo},T} = 1789$ m/s and $\eta_T = 0.25$ ($V_{P0,T} = 2000$ m/s, $\epsilon_T = 0.1$, and $\delta_T = -0.1$). Migration was done with the parameters $V_{\mathrm{nmo},M} = V_{\mathrm{nmo},T} = 1789$ m/s and $\eta_M = 0.4$ ($V_{P0,M} = 1789$ m/s, $\epsilon_M = 0.4$, and $\delta_M = 0$). In the true model the image point has a maximum offset-to-depth ratio of two.

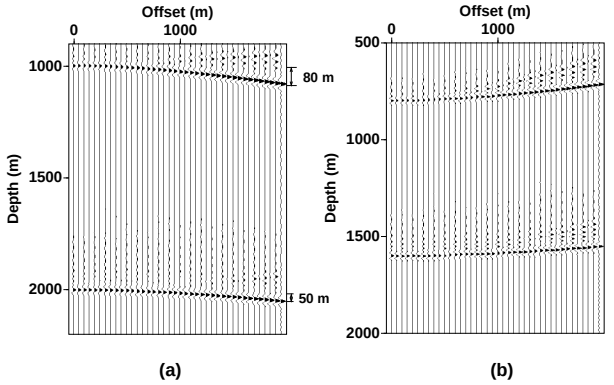

Figure 4. Image gathers for two horizontal reflectors computed for inaccurate values of the NMO velocity. The true parameters are the same as in Figure 3: $V_{\mathrm{nmo},T} = 1789$ m/s and $\eta_T = 0.25$. Migration was done with the correct η and (a) $V_{\mathrm{nmo},M} = 2000$ m/s ($V_{P0,M} = 2000$ m/s, $\epsilon_M = 0.25$ and $\delta_M = 0$); (b) $V_{\mathrm{nmo},M} = 1600$ m/s ($V_{P0,M} = 1600$ m/s, $\epsilon_M = 0.25$ and $\delta_M = 0$). In the true model, the maximum offset-to-depth ratio $x_{\max}/z = 2$ for the shallow reflector and $x_{\max}/z = 1$ for the deep reflector.

on the zero-offset traveltime, V_{nmo} and η. Positioning an image gather at the true depth, however, requires using the correct vertical velocity ($V_{P0,M} = V_{P0,T}$, which makes $\gamma = 1$).

Figure 1a shows image gathers for two horizontal reflectors embedded in a homogeneous VTI medium at depths of 1000 m and 2000 m. The gathers were computed for a model with the true parameters $V_{\mathrm{nmo},T} = V_{\mathrm{nmo},M}$ and $\eta_M = \eta_T$, but intentionally inaccurate values of the vertical velocity V_{P0} and the coefficients ϵ and δ. Evidently, setting V_{nmo} and η to the correct values ensures that both image gathers are flat. The same conditions ($V_{\mathrm{nmo},T} = V_{\mathrm{nmo},M}$ and $\eta_M = \eta_T$) are sufficient to flatten image gathers for dipping reflectors in Figure 1b.

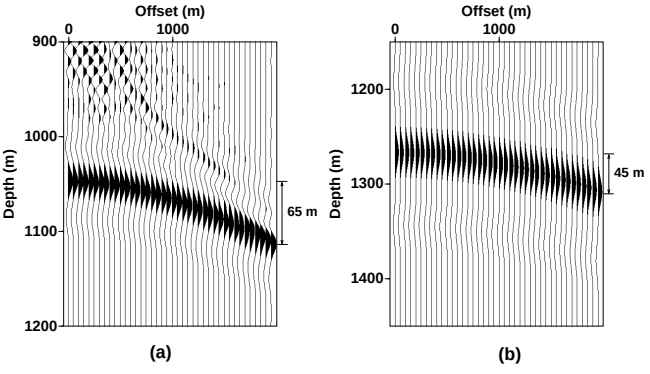

Figure 5. Image gathers for reflectors dipping at (a) 30° and (b) 45° computed for an overstated value of V_{nmo}. The true parameters are the same as in Figure 3: $V_{\mathrm{nmo},T} = 1789$ m/s and $\eta_T = 0.25$. Migration was done with the correct η and $V_{\mathrm{nmo},M} = 2000$ m/s ($V_{P0,M} = 2000$ m/s, $\epsilon_M = 0.25$ and $\delta_M = 0$). In the true model the image point has a maximum offset-to-depth ratio of two.

However, since the migration was performed with the wrong value of V_{P0}, the migrated depths are scaled by the factor $\gamma \approx 0.90$. In agreement with equation (5), the depth of the shallow image gather is 900 m instead of 1000 m, and the deep image gather is located at 1800 m instead of 2000 m.

In equation (5), the parameter η contributes only to the quartic moveout term h^4, which is also the case for the P-wave nonhyperbolic reflection moveout equation (Alkhalifah and Tsvankin, 1995; Tsvankin, 2001). Therefore, the influence of η is expected to be substantial only for relatively large offset-to-depth ratios exceeding unity. Indeed, the error in η in Figure 2 ($\eta_M - \eta_T = \pm 0.15$) does not cause a visible residual moveout on the image gather of the deeper event, for which the maximum offset-to-depth ratio $x_{\max}/z$ is equal to unity. In contrast, the gather of the shallow event ($x_{\max}/z = 2$) exhibits substantial distortions at larger offsets. If the value of η is too high, the migrated depth z increases with offset h (Figure 2a), while if η is too small, $z(h)$ decreases for large h (Figure 2b).

For dipping reflectors, the parameter η contributes to small-offset traveltimes as well because it governs the dip dependence of NMO velocity (Alkhalifah and Tsvankin, 1995; Tsvankin, 2001). Figure 3 confirms that for dipping events (the dips are 30° and 45°) the residual moveout caused by errors in η is not confined to long offsets. The depth error at the largest offset increases from 30 m for the horizontal reflector (Figure 2a) to 50 m for the reflector dipping at 30° (Figure 3a), but then decreases to 35 m for a dip of 45° (Figure 3b); this behavior of residual moveout agrees with the prediction

of Jaramillo and Larner (1995). Although the contribution of η to the NMO velocity becomes more significant with dip, the magnitude of reflection moveout decreases for steeper reflectors, which explains this dependence of residual moveout on errors in η.

The NMO velocity in equation (5) not only controls the quadratic term h^2 that dominates the moveout for offsets used in our examples, but also influences the quartic term h^4. Hence, an inaccurate value of $V_{\rm nmo}$ in Figures 4 and 5 ($|V_{{\rm nmo},M} - V_{{\rm nmo},T}| \approx 200$ m/s) leads to significant residual moveout for the whole offset range. The depth error at the largest offset reaches 80 m for a horizontal reflector (Figure 4a) and decreases to 65 m for the 30° reflector (Figure 5a), and to 45 m for a dip of 45° (Figure 5b). This steady decrease in residual moveout with dip for a fixed error in $V_{\rm nmo}$ is caused by the smaller magnitude of reflection moveout and its lower sensitivity to $V_{\rm nmo}$ for steeper dips. Liu (1995) noticed this phenomenon for isotropic media, and his analysis remains qualitatively valid in the presence of anisotropy.

Factorized $v(z)$ VTI medium

Factorized $v(z)$ VTI models have constant values of the anisotropic parameters and spatially varying vertical velocities of P- and S-waves (e.g., Červený, 1989). We consider a subset of factorized VTI models with a linear dependence of the vertical velocity V_{P0} on the coordinates x and z. This section is devoted to vertically heterogeneous models of this type, in which kinematic signatures of P-waves are defined by the velocity V_{P0} at the surface ($z = 0$), the vertical-velocity gradient k_z and the parameters ϵ and δ.

As discussed in Appendix B, an image gather at the zero-offset time t_0 can be flattened by using the correct values of the effective NMO velocity and the effective parameter $\hat{\eta}$ given by

$$v^2_{\rm nmo}(t_0) \quad = \quad \frac{V^2_{P0}(1+2\delta)}{t_0\, k_z}\, \left[e^{k_z\, t_0} - 1\right] , \qquad (6)$$

$$\hat{\eta}(t_0) = \frac{1}{8}\left\{ \frac{(1+8\eta)\,(e^{2k_z\, t_0} - 1)\, k_z\, t_0}{2(e^{k_z t_0} - 1)^2} - 1 \right\} . \qquad (7)$$

However, since the vertical velocity in a factorized $v(z)$ medium changes with depth, flattening an image gather for a certain depth z_T does not ensure that the same model will flatten gathers for any other depth. To illustrate this point, consider two horizontal reflectors at the depths 1000 m and 2000 m embedded in a factorized $v(z)$ medium (Figure 6). To migrate data acquired over such a model, we use a homogeneous VTI medium with the parameters chosen in such a way that $V_{\rm nmo}$ for the homogeneous model is equal to the NMO velocity

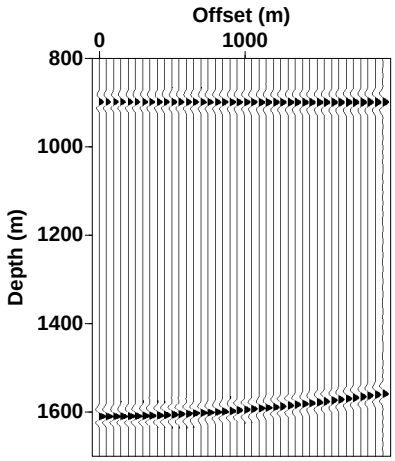

Figure 6. Image gathers for two horizontal reflectors in a factorized $v(z)$ VTI medium obtained using a homogeneous migration model with the correct value of η and the NMO velocity equal to that for the shallow reflector. The true parameters are $V_{P0,T} = 2000$ m/s, $k_{z,T} = 0.6$ 1/s, $\epsilon_T = 0.1$ and $\delta_T = -0.1$; the parameters used for the migration are $V_{P0,M} = 2054$ m/s, $k_{z,M} = 0$, $\epsilon_M = 0.26$ and $\delta_M = 0$.

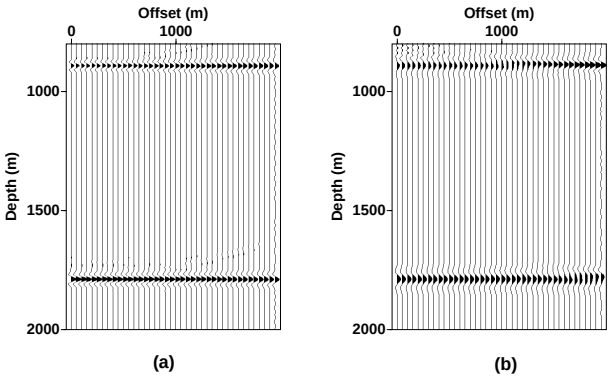

Figure 7. Image gathers for (a) two horizontal reflectors and (b) two reflectors dipping at 30° embedded in a factorized VTI medium. The model parameters are $V_{P0,T} = 2000$ m/s, $k_{z,T} = 0.6$ 1/s, $\epsilon_T = 0.1$ and $\delta_T = -0.1$. Prestack depth migration was performed for a different model that has the correct $V_{{\rm nmo},M} = V_{{\rm nmo},T} = 1789$ m/s, $k_{z,M} = k_{z,T} = 0.6$ 1/s, and $\eta_M = \eta_T = 0.25$ ($V_{P0,M} = 1789$ m/s, $k_{z,M} = 0.6$ 1/s, $\epsilon_M = 0.25$ and $\delta_M = 0$). In the true model, the maximum offset-to-depth ratio $x_{\rm max}/z = 2$ for the shallow reflector and $x_{\rm max}/z = 1$ for the deep reflector.

for the shallow reflector, $v_{{\rm nmo},M}[z_M(0)] = v_{{\rm nmo},T}(1000)$, and $\hat{\eta}_M[z_M(0)] = \hat{\eta}_T(1000) = 0.26$. As expected, the image gather for the shallow reflector is flat, but the gather for the deep reflector exhibits substantial residual moveout because the NMO velocity and $\hat{\eta}$ used in migration are too low for a depth of 2000 m.

To ensure that image gathers are flat for the whole

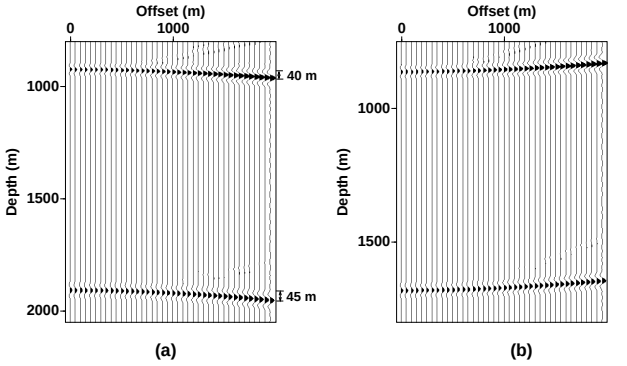

Figure 8. Image gathers for two horizontal reflectors computed for inaccurate values of the vertical velocity gradient. The true parameters are $V_{P0,T} = 2000$ m/s, $k_{z,T} = 0.6$ 1/s, $\epsilon_T = 0.1$ and $\delta_T = -0.1$. Migration was done with the correct $V_{\mathrm{nmo},M} = V_{\mathrm{nmo},T}$ and $\eta_M = \eta_T$, but distorted values of $k_{z,M}$. (a) $k_{z,M} - k_{z,T} = 0.15$ ($V_{P0,M} = 1789$ m/s, $k_{z,M} = 0.75$ 1/s, $\epsilon_M = 0.25$ and $\delta_M = 0$). (b) $k_{z,M} - k_{z,T} = -0.15$ ($V_{P0,M} = 1789$ m/s, $k_{z,M} = 0.45$ 1/s, $\epsilon_M = 0.25$ and $\delta_M = 0$). In the true model, the maximum offset-to-depth ratio $x_{\max}/z = 2$ for the shallow reflector and $x_{\max}/z = 1$ for the deep reflector.

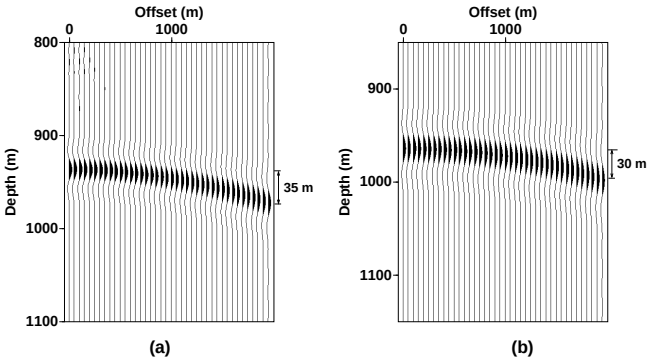

Figure 9. Image gathers for reflectors dipping at (a) 30° and (b) 45° computed for a value of k_z overstated by 0.15. The true parameters are $V_{P0,T} = 2000$ m/s, $k_{z,T} = 0.6$ 1/s, $\epsilon_T = 0.1$ and $\delta_T = -0.1$. Migration was done with the parameters $V_{P0,M} = 1789$ m/s, $k_{z,M} = 0.75$ 1/s, $\epsilon_M = 0.25$ and $\delta_M = 0$. In the true model the image point has a maximum offset-to-depth ratio of two.

depth range occupied by the reflectors, the effective NMO velocity and the parameter $\hat{\eta}$ for the migration and true models should be equal at all zero-offset times t_0. Therefore, both the exponential term in equation (6) and the coefficient in front of it should be preserved in the migration model, which means that migration should be done with the correct values of the vertical velocity gradient and the NMO velocity at the surface: $k_{z,M} = k_{z,T}$ and $V_{\mathrm{nmo},M} = V_{P0,M}\sqrt{1+2\delta_M} = V_{P0,T}\sqrt{1+2\delta_T} = V_{\mathrm{nmo},T}$. Taking into account that $k_{z,M}$ has to be equal to $k_{z,T}$, the condition $\hat{\eta}_M = \hat{\eta}_T$ can be satisfied at all t_0 only if $\eta_M = \eta_T$ [see equation (7)].

We conclude that to flatten gathers of all horizontal events in a factorized $v(z)$ medium, three conditions need to be satisfied: (1) $V_{\mathrm{nmo},M} = V_{\mathrm{nmo},T}$, (2) $k_{z,M} = k_{z,T}$, and (3) $\eta_M = \eta_T$. Although in principle all three conditions follow from the general result of Alkhalifah and Tsvankin (1995), the formulation given here for factorized VTI media is new. In particular, we showed that flattening image gathers for a range of zero-offset times requires using the correct vertical velocity gradient k_z. This implies that velocity analysis on image gathers in VTI media may be used to constrain not just parameters η and V_{nmo} (as expected), but also the gradient k_z.

Figure 7a confirms that if the parameters V_{nmo}, k_z, and η are the same for the migration and true models (although the Thomsen parameters of those models may differ), image gathers of horizontal events are flat. Moreover, these three conditions are also sufficient to flatten image gathers of dipping events (Figure 7b).

The image gather for a horizontal reflector embedded in a factorized $v(z)$ VTI medium can be described by the following equation (Appendix B):

$$\begin{aligned} z_M^2(h) \;\approx\; & z_M^2(0) \\ & - h^2 \hat{V}_{P0,M}^2 \left\{ \frac{1}{v_{\mathrm{nmo},M}^2[z(0)]} - \frac{1}{v_{\mathrm{nmo},T}^2(z_T)} \right\} \\ & + 2\frac{h^4}{h^2+z_T^2} \left\{ \hat{\eta}_M \frac{v_{\mathrm{nmo},M}^2[z(0)]}{v_{\mathrm{nmo},T}^2(z_T)} \right. \\ & \left. - \hat{\eta}_T \frac{v_{\mathrm{nmo},T}^2(z_T)}{v_{\mathrm{nmo},M}^2[z(0)]} \right\}. \end{aligned} \tag{8}$$

Here, $z_M(0) = \gamma z_T$, $\gamma \equiv \hat{V}_{P0,M}/\hat{V}_{P0,T}$, and $\hat{V}_{P0}$ is the average vertical velocity above the reflector. Equation (8), obtained under the assumption that vertical heterogeneity can be neglected on the depth scale of the image gather, has the same form as the corresponding expression (5) for homogeneous media. Note that the reflector depth is scaled by the factor γ, which in heterogeneous media depends on the ratio of the average vertical velocities in the migration and true models. Indeed, the depths in Figure 7 are about 10% smaller than those in the true model ($\gamma \approx 0.9$).

Because of the similarity between equations (5) and (8), the influence of errors in V_{nmo} or η on image gathers in factorized $v(z)$ media resembles that for homogeneous media. Therefore, here we focus on the sensitivity of image gathers to the gradient k_z in factorized $v(z)$ media. Figure 8 illustrates the distortions of image gathers of horizontal events resulting from errors in k_z. An increase in k_z leads to a higher NMO velocity, and the image gather bends towards larger depths (Figure 8a), while choosing $k_{z,M} < k_{z,T}$ is equivalent to understating the NMO velocity (Figure 8b). Since an erroneous k_z causes the corresponding error in the vertical velocity to

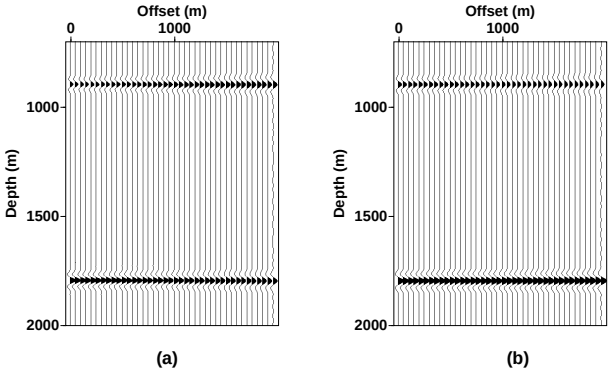

Figure 10. Image gathers for (a) two horizontal reflectors and (b) two reflectors dipping at 30° embedded in a factorized $v(x,z)$ VTI medium. In Figures 10–15 the true model parameters are $V_{P0,T} = 2000$ m/s, $k_{z,T} = 0.6$ 1/s, $k_{x,T} = 0.2$ 1/s, $\epsilon_T = 0.1$ and $\delta_T = -0.1$. Prestack depth migration was performed for a different model that has the correct $V_{\mathrm{nmo},M} = V_{\mathrm{nmo},T} = 1789$ m/s, $k_{z,M} = k_{z,T} = 0.6$ 1/s, $k_{x,M}\sqrt{1+2\delta_M} = k_{x,T}\sqrt{1+2\delta_T} = 0.18$ 1/s, and $\eta_M = \eta_T = 0.25$ ($V_{P0,M} = 1789$ m/s, $k_{z,M} = 0.6$ 1/s, $k_{x,M} = 0.18$ 1/s, $\epsilon_M = 0.25$ and $\delta_M = 0$). In the true model, the maximum offset-to-depth ratio $x_{\max}/z = 2$ for the shallow reflector and $x_{\max}/z = 1$ for the deep reflector.

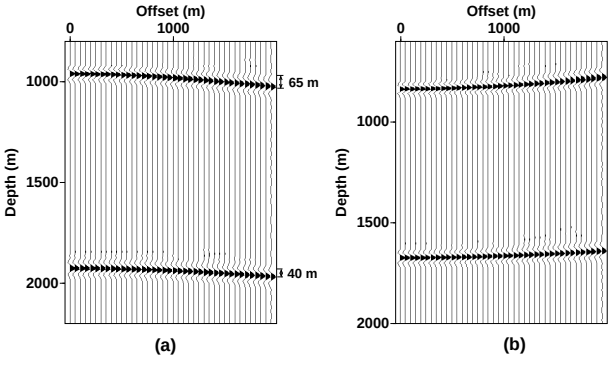

Figure 11. Image gathers for two horizontal reflectors computed for inaccurate values of V_{nmo}, but correct $\eta_M = \eta_T = 0.25$, $k_{z,M} = k_{x,T} = 0.6$ 1/s and $k_{x,M}\sqrt{1+2\delta_M} = k_{x,T}\sqrt{1+2\delta_T} = 0.18$ 1/s. (a) $V_{\mathrm{nmo},M} - V_{\mathrm{nmo},T} \approx 200$ m/s ($V_{P0,M} = 2000$ m/s, $k_{z,M} = 0.6$ 1/s, $k_{x,M} = 0.18$ 1/s, $\epsilon_M = 0.25$ and $\delta_M = 0$). (b) $V_{\mathrm{nmo},M} - V_{\mathrm{nmo},T} \approx -200$ m/s ($V_{P0,M} = 1600$ m/s, $k_{z,M} = 0.6$ 1/s, $k_{x,M} = 0.18$ 1/s, $\epsilon_M = 0.25$, and $\delta_M = 0$). In the true model, the maximum offset-to-depth ratio $x_{\max}/z = 2$ for the shallow reflector and $x_{\max}/z = 1$ for the deep reflector.

increase with depth, the residual moveout in Figure 8 is more substantial for the deep gather.

The influence of k_z on image gathers of dipping events is shown in Figure 9. For a fixed error (0.15 1/s) in k_z, the residual moveout decreases from 40 m for the shallow horizontal reflector (Figure 8a) to 35 m for a dip of 30° to 30 m for a dip of 45°. This dip dependence of residual moveout is similar to that observed in a homogeneous medium for a fixed error in V_{nmo}.

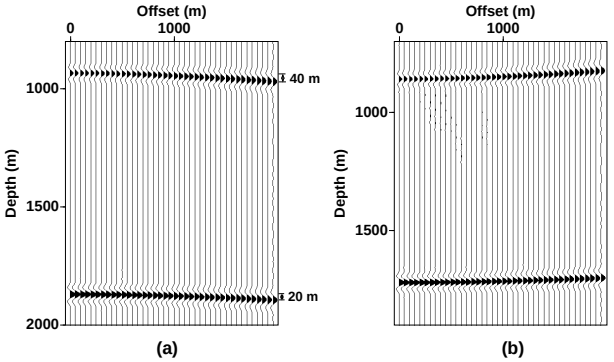

Figure 12. Image gathers for two horizontal reflectors computed for inaccurate values of $k_x\sqrt{1+2\delta}$, but correct $V_{\mathrm{nmo},M} = V_{\mathrm{nmo},T} = 1789$ m/s, $k_{z,M} = k_{z,T}$, and $\eta_M = \eta_T = 0.25$. (a) $k_{x,M}\sqrt{1+2\delta_M} - k_{x,T}\sqrt{1+2\delta_T} = 0.02$ ($V_{P0,M} = 1789$ m/s, $k_{z,M} = 0.6$ 1/s, $k_{x,M} = 0.20$ 1/s, $\epsilon_M = 0.25$, and $\delta_M = 0$). (b) $k_{x,M}\sqrt{1+2\delta_M} - k_{x,T}\sqrt{1+2\delta_T} = -0.02$ ($V_{P0,M} = 1789$ m/s, $k_{z,M} = 0.6$ 1/s, $k_{x,M} = 0.16$ 1/s, $\epsilon_M = 0.25$, and $\delta_M = 0$). The gathers are centered at a location 6000 m away from $x = 0$. In the true model, the maximum offset-to-depth ratio $x_{\max}/z = 2$ for the shallow reflector and $x_{\max}/z = 1$ for the deep reflector.

Factorized $v(x,z)$ VTI medium

Factorized $v(x,z)$ VTI media with linear velocity variation can be described by five independent parameters: the vertical velocity $V_{P0} = V_{P0}(0,0)$ defined at zero depth and lateral location $x = 0$, the velocity gradients k_x and k_z responsible for the linear variation of V_{P0} in the x– and z–directions, respectively, and Thomsen parameters ϵ and δ (for P-waves). In principle, we can treat a factorized $v(x,z)$ model as being composed of narrow vertical strips of $v(z)$ factorized media discussed above. Therefore, it is natural to assume that image gathers in $v(x,z)$ media will be flat if $v_{\mathrm{nmo},M}[x,t_0(x)] = v_{\mathrm{nmo},T}[x,t_0(x)]$ and $\hat{\eta}_M[x,t_0(x)] = \hat{\eta}_T[x,t_0(x)]$ not only for all vertical times t_0, but also for all coordinates x.

The influence of weak lateral velocity variation on the NMO velocity in horizontally layered anisotropic media was discussed by Grechka and Tsvankin (1999). They showed that the NMO ellipse has to be corrected for lateral velocity variation by including a term dependent on the *second* derivatives of the vertical velocity with respect to the horizontal coordinates. For P-waves in the 2-D model considered here, the equation of Grechka and Tsvankin (1999) takes the form

$$v_{\mathrm{nmo}}^{-2}(x,z) = v_{\mathrm{nmo,hom}}^{-2}(x,z) + \frac{\tau_0(x,z)}{3}\,\frac{\partial^2\tau_0(x,z)}{\partial x^2}, \quad (9)$$

where $v_{\mathrm{nmo,hom}}$ is the NMO velocity in the background laterally homogeneous medium at the coordinate x, z

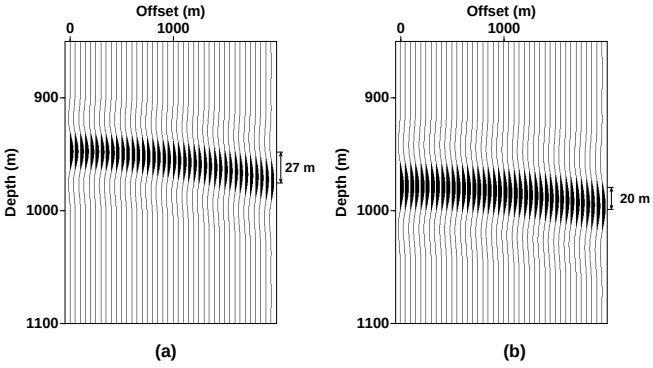

Figure 13. Image gathers for reflectors dipping at (a) 30° and (b) 45° computed for a value of $k_x\sqrt{1+2\delta}$ overstated by 0.02, but correct $V_{\mathrm{nmo},M} = V_{\mathrm{nmo},T} = 1789$ m/s, $k_{z,M} = k_{z,T}$, and $\eta_M = \eta_T = 0.25$ ($V_{P0,M} = 1789$ m/s, $k_{z,M} = 0.6$ 1/s, $k_{x,M} = 0.2$ 1/s, $\epsilon_M = 0.25$, and $\delta_M = 0$). The gathers are centered at a location 6000 m away from $x = 0$. In the true model the image point has a maximum offset-to-depth ratio of two.

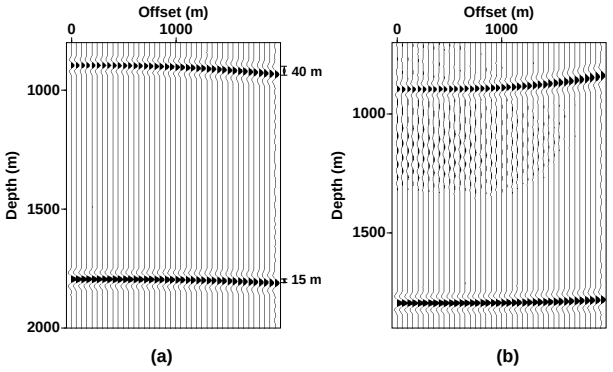

Figure 14. Image gathers for two horizontal reflectors computed for inaccurate values of η, but correct $V_{\mathrm{nmo},M} = V_{\mathrm{nmo},T} = 1789$ m/s, $k_{z,M} = k_{z,T}$, and $k_{x,M}\sqrt{1+2\delta_M} = k_{x,T}\sqrt{1+2\delta_T}$. (a) $\eta_M - \eta_T = 0.15$ ($V_{P0,M} = 1789$ m/s, $k_{z,M} = 0.6$ 1/s, $k_{x,M} = 0.18$ 1/s, $\epsilon_M = 0.4$, and $\delta_M = 0$). (b) $\eta_M - \eta_T = -0.15$ ($V_{P0,M} = 1789$ m/s, $k_{z,M} = 0.6$ 1/s, $k_{x,M} = 0.18$ 1/s, $\epsilon_M = 0.1$, and $\delta_M = 0$). In the true model, the maximum offset-to-depth ratio $x_{\max}/z = 2$ for the shallow reflector and $x_{\max}/z = 1$ for the deep reflector.

is the reflector depth and $\tau_0(x,z)$ is the one-way zero-offset reflection traveltime. Since in our model $V_{P0}(x,z)$ [and, for weak lateral velocity variation, $\tau_0(x,z)$] is a linear function of x, $v_{\mathrm{nmo}}(x,z)$ from equation (9) is simply equal to the NMO velocity in the background factorized $v(z)$ medium at the lateral location x. Using equation (B5), the background NMO velocity can be represented as

$$v^2_{\mathrm{nmo,hom}}(x) = \frac{V^2_{P0}(x)(1+2\delta)}{2\,t_{\mathrm{hom}}(x)\,k_z}\left[e^{2k_z t_{\mathrm{hom}}(x)} - 1\right], \quad (10)$$

where $V_{P0}(x) = V_{P0} + k_x x$, $t_{\mathrm{hom}}(x) = z_T/\hat{V}_{P0}(x)$, and

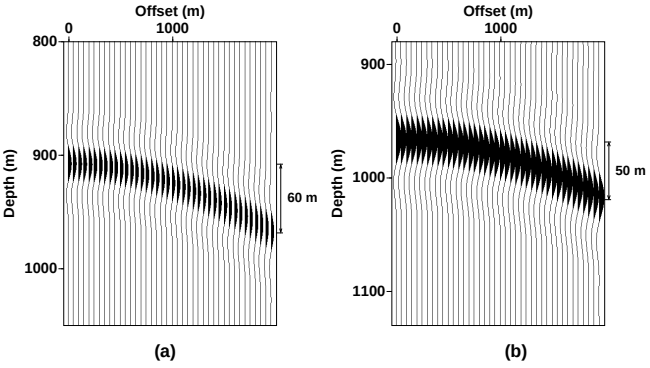

Figure 15. Image gathers for reflectors dipping at (a) 30° and (b) 45° computed for a value of η overstated by 0.15, but correct $V_{\mathrm{nmo},M} = V_{\mathrm{nmo},T} = 1789$ m/s, $k_{z,M} = k_{z,T}$, and $k_{x,M}\sqrt{1+2\delta_M} = k_{x,T}\sqrt{1+2\delta_T}$ ($V_{P0,M} = 1789$ m/s, $k_{z,M} = 0.6$ 1/s, $k_{x,M} = 0.18$ 1/s, $\epsilon_M = 0.4$, and $\delta_M = 0$). In the true model the image point has a maximum offset-to-depth ratio of two.

$\hat{V}_{P0}(x,z)$ is the average vertical velocity above the reflector.

As follows from our results for the $v(z)$ model, v_{nmo} of horizontal events are equal to the true NMO velocities for all vertical times t_0 if the migration is based on the correct values of the vertical velocity gradient k_z and the NMO velocity at the surface $[V_{P0}(x)\sqrt{1+2\delta}]$. Hence, $k_{z,M}$ should be equal to $k_{z,T}$, and

$$(V_{P0,M} + k_{x,M}\,x)\sqrt{1+2\delta_M} = (V_{P0,T} + k_{x,T}\,x)\sqrt{1+2\delta_T}\,, \quad (11)$$

which implies that $V_{\mathrm{nmo},M} = V_{P0,M}\sqrt{1+2\delta_M} = V_{P0,T}\sqrt{1+2\delta_T} = V_{\mathrm{nmo},T}$ and $k_{x,M}\sqrt{1+2\delta_M} = k_{x,T}\sqrt{1+2\delta_T}$. Also, because $k_{z,M} = k_{z,T}$, setting $\hat{\eta}_M[x, t_0(x)] = \hat{\eta}_T[x, t_0(x)]$ for all zero-offset times and lateral positions implies that $\eta_M = \eta_T$.

We conclude that flattening all image gathers in a factorized $v(x,z)$ medium requires satisfying four conditions:
(1) $V_{\mathrm{nmo},M} = V_{\mathrm{nmo},T}$,
(2) $k_{z,M} = k_{z,T}$,
(3) $\eta_M = \eta_T$, and
(4) $k_{x,T}\sqrt{1+2\delta_T} = k_{x,M}\sqrt{1+2\delta_M}$.
The first three conditions coincide with those obtained for $v(z)$ media, and (4) is an additional constraint on the horizontal velocity gradient combined with the parameter δ. Thus, while it may be possible to estimate the vertical gradient k_z from image gathers, the individual values of the horizontal gradient k_x and the parameters V_{P0}, ϵ, and δ cannot be found using P-wave reflection moveout alone.

As illustrated by Figure 10a, the conditions listed above indeed ensure that the image gathers of horizon-

tal events are flat, even if the migration is done with erroneous model parameters. Although equation (10) was derived for horizontal reflectors, the same four conditions are sufficient for flattening image gathers of dipping events (Figure 10b). However, because an incorrect vertical velocity was used, the depths are stretched by the factor equal to the ratio of the migration $[\hat{V}_{P0,M}(x)]$ and true $[\hat{V}_{P0,T}(x)]$ average vertical velocities evaluated at the CMP coordinate x. For the examples in Figure 10, the reflector depths are underestimated by about 10%.

To flatten image gathers for a *single* horizontal event, $v_{\rm nmo}(x, z_T)$ must be equal to $v_{\rm nmo}[x, z_M(0)]$ for all x, but only for one vertical time t_0. Using a single event, it is impossible to constrain the vertical velocity gradient because of the trade-off between k_z and the NMO velocity at the surface. In general, removing the residual moveout in an image gather at a certain depth does not guarantee that image gathers at other depths will be flat, unless independent information about the vertical gradient is available.

Inaccurate values of $V_{\rm nmo}$, k_z, or $k_x\sqrt{1+2\delta}$ cause an error in $v_{\rm nmo}$ and residual moveout on image gathers for the whole offset range. Figures 11–13 show the influence of errors in $V_{\rm nmo}$ and $k_x\sqrt{1+2\delta}$, while errors in k_z were analyzed above for $v(z)$ media (Figures 8 and 9). The image gathers are particularly sensitive to the horizontal velocity gradient k_x, with an error in $k_x\sqrt{1+2\delta}$ of just 0.02 1/s (that translates into an error of 100 m/s in the vertical velocity) creating a substantial residual moveout (Figures 12 and 13). As in homogeneous media, the residual moveout for a fixed error in one of the three parameters listed above decreases with reflector dip (e.g., see Figures 12a and 13).

It is noteworthy that the magnitude of residual moveout caused by a fixed error in $V_{\rm nmo}$ is smaller in factorized media than in homogeneous media for the same $V_{P0,M}$, $V_{P0,T}$, ϵ_M, ϵ_T, δ_M, and δ_T. For example, if the value of $V_{\rm nmo}$ is overstated by 200 m, the residual moveout for the shallow horizontal reflector embedded in a homogeneous VTI medium reaches 80 m (Figure 4a). If the same reflector is embedded in a factorized $v(x,z)$ VTI medium, the residual moveout is limited to 65 m (Figure 11b). Therefore, velocity gradients tend to mitigate the distortions of image gathers caused by errors in $V_{\rm nmo}$. Likewise, the residual moveout for a fixed error in k_z is smaller in a $v(x,z)$ medium than in the corresponding laterally homogeneous $v(z)$ model.

In contrast, the residual moveout associated with errors in η is larger for factorized $v(x,z)$ media than for the corresponding homogeneous medium. If η is distorted by 0.15, the residual moveout increases from 30 m for a homogeneous medium (Figure 2a) to 40 m for a factorized $v(x,z)$ medium (Figure 14a). The dip dependence of the residual moveout in factorized media for a fixed error in η has the same character as in homogeneous media. For a 0.15 error in η, the residual increases from 40 m for a horizontal reflector (Figure 14a) to 60m for a reflector dipping at 30° (Figure 15a), and then decreases to 50 m for a 45° dip (Figure 15b).

Discussion and conclusions

In conventional seismic processing for isotropic media, image gathers proved to be a convenient tool for refining velocity models as well as for a quick qualitative assessment of the accuracy of velocity analysis. If the medium is anisotropic, reflection moveout is governed by several anisotropic parameters, and the interpretation of image gathers becomes much more complicated. Here, we presented an analytic and numerical study of P-wave image gathers in homogeneous and factorized [$v(z)$ and $v(x,z)$] VTI media.

Using the weak-anisotropy approximation, we obtained a simple representation of image gathers of horizontal events for homogeneous VTI media in terms of the vertical velocity V_{P0}, the NMO velocity $V_{\rm nmo}$ and the Alkhalifah-Tsvankin parameter η. Although the equation of an image gather is derived in the depth domain, its structure is similar to that of the nonhyperbolic equation for P-wave reflection traveltimes (Tsvankin and Thomsen, 1994; Alkhalifah and Tsvankin, 1995). The moveout on image gathers depends on the parameters $V_{\rm nmo}$ and η, with the NMO velocity responsible for the small-offset term and η governing the term quartic in offset. Therefore, although in principle the correct values of both $V_{\rm nmo}$ and η are needed to flatten a gather, the influence of η becomes substantial only for offset-to-depth ratios exceeding unity.

In agreement with the general result of Alkhalifah and Tsvankin (1995), the same conditions (correct values of $V_{\rm nmo}$ and η) are needed to flatten image gathers of dipping events, but in the presence of dip η makes a substantial contribution to the near-offset moveout as well. The magnitude of residual moveout for a fixed error in $V_{\rm nmo}$ decreases with dip, while the residuals caused by an error in η reach their maximum value for intermediate dips (25–35° in our examples). Even if prestack migration is performed with the correct parameters $V_{\rm nmo}$ and η and the image gathers are flat and well focused, the depth is scaled by a "stretching" factor equal to the ratio of the migration and true vertical velocities.

For factorized $v(z)$ models with a constant vertical velocity gradient k_z, the equation for image gathers of horizontal events has the same form as that in homoge-

neous media, but it contains the effective vertical and NMO velocities. Flattening image gathers of events with any dip in $v(z)$ media requires the correct values of the NMO velocity at the surface, the coefficient η and the gradient k_z. The influence of errors in k_z on the residual moveout decreases with dip (as is the case for errors in $V_{\rm nmo}$) but increases with reflector depth.

Extension of the above results to laterally heterogeneous $v(x,z)$ models is based on the NMO equation of Grechka and Tsvankin (1999) that includes a correction term dependent on the lateral variation of the vertical velocity (or vertical traveltime). For a weak linear velocity dependence on x, the correction term vanishes, and the NMO velocity is equal to the corresponding value in the laterally homogeneous background. To equalize the background NMO velocities for all x, migration should be done with the correct value of the parameter combination $k_x\sqrt{1+2\delta}$ (k_x is the horizontal velocity gradient).

Therefore, moveout on image gathers in $v(x,z)$ media is controlled by four parameter combinations – $V_{P0}\sqrt{1+2\delta}$, η, k_z, and $k_x\sqrt{1+2\delta}$. A positive error in any of these quantities causes the image gathers to curve down (i.e., the depth increases with offset) and a negative error causes the gathers to curve up. For a fixed error in $V_{P0}\sqrt{1+\delta}$, the residual moveout in $v(x,z)$ media is smaller than that in the reference homogeneous model, which indicates that lateral heterogeneity is likely to hamper the estimation of this parameter from image gathers. In contrast, the influence of η on image gathers becomes more substantial in the presence of lateral heterogeneity, and errors in η lead to measurable residual moveout of horizontal events for offset-to-depth ratios close to unity.

Estimation of these four key parameter combinations requires using several image gathers at different depths and lateral positions, which will be discussed in detail in a sequel paper. Even if all four combinations have been resolved, separation of lateral velocity variation from the anisotropic coefficients cannot be accomplished without additional information. Indeed, the lateral velocity gradient cannot be decoupled from anisotropy because it contributes to moveout on image gathers only through the factor $k_x\sqrt{1+2\delta}$.

It is important to emphasize, however, that the vertical velocity gradient k_z is constrained not only in the $v(z)$ model, but also in laterally heterogeneous media. As a result, although the inversion of P-wave data for the vertical velocity and Thomsen coefficients will suffer from inherent ambiguities, minimal *a priori* assumptions may be sufficient to remove the trade-offs between the VTI parameters. For example, if the vertical velocity V_{P0} is known at any single surface location (which is quite possible), then the inverted gradient k_z can be used to reconstruct the function $V_{P0}(z)$ and find the depth scale of the model. Also, in this case the anisotropic parameter δ can be determined from the NMO velocity at the surface ($V_{P0}\sqrt{1+2\delta}$), and, in turn, used to estimate the horizontal gradient k_x from the combination $k_x\sqrt{1+2\delta}$. The sequel paper will examine the feasibility of this parameter-estimation methodology for different sets of input data and realistic levels of noise.

References

Alkhalifah, T., 1995, Gaussian beam depth migration for anisotropic media: Geophysics, **60**, 1474-1484.

Alkhalifah, T. 1996, Seismic processing in transversely isotropic media: PhD thesis, Colorado School of Mines.

Alkhalifah, T. and Tsvankin, I., 1995, Velocity analysis for transversely isotropic media: Geophysics, **60**,1550-1566.

Alkhalifah, T., Tsvankin, I., Larner, K., and Toldi, J., 1996, Velocity analysis and imaging in transversely isotropic media: Methodology and a case study: The Leading Edge, **15**, no. 5, 371–378.

Al-Yahya, K., 1987, Prestack migration velocity analysis: Determination of interval velocities, SEP-51, 49-61.

Brandsberg-Dahl, S. 2001, Imaging-inversion and migration velocity analysis in the scattering-angle/azimuth domain: Ph.D. thesis, Colorado School of Mines.

Banik, N.C., 1984, Velocity anisotropy of shales and depth estimation in the North Sea basin: Geophysics, **49**, 1411-1419.

Červený, V., 1989, Ray tracing in factorized anisotropic inhomogeneous media: Geophys. J. Intl., **99**, 91-100.

Gajewski, D. and Pšenčík, I., 1987, Computation of high-frequency seismic wavefields in 3-D laterally inhomogeneous anisotropic media: Geophys. J. R. Astr. Soc., **91**, 383-411.

Grechka, V. and Tsvankin, I., 1999, 3-D moveout inversion in azimuthally anisotropic media with lateral velocity variation: Theory and a case study: Geophysics, **64**, 1202-1218.

Jaramillo, H. and Larner, K., 1995, Prestack migration error in transversely isotropic media: CWP Research Report (CWP-185).

Liu, Z., 1995, Migration velocity analysis: PhD thesis, Colorado School of Mines.

Meng, Z., 1999, Tetrahedral based earth models, ray tracing in tetrahedral models and analytical migration velocity analysis: PhD thesis, Colorado School of Mines.

Peng, C. and Steenson, K.E., 2001, 3-D prestack depth migration in anisotropic media: A case study at the

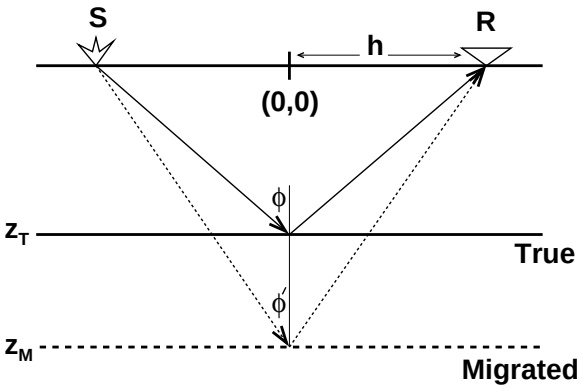

Figure A1. True and migrated positions of a horizontal reflector.

Lodgepole reef play in North Dakota: The Leading Edge, **20**, 524-527.

Stork, C., 1991, Reflection tomography in the post migrated domain: Geophysics, **57**, 680-692.

Thomsen, L., 1986, Weak elastic anisotropy: Geophysics, **51**, 1954-1966.

Tsvankin, I., 2001, Seismic signatures and and analysis of reflection data in anisotropic media: Elsevier.

Tsvankin, I. and Thomsen, L., 1994, Nonhyperbolic reflection moveout in anisotropic media: Geophysics, **59**, 1290-1304.

Zhu, J., Lines, L. and Gray, S., 1998, Smiles and frowns in migration velocity analysis: Geophysics, **63**, 1200-1209.

APPENDIX A: Image gather for a horizontal reflector in a homogeneous VTI medium

Consider a horizontal reflector located at the depth z_T in a VTI medium with the vertical velocity $V_{P0,T}$ and Thomsen parameters ϵ_T and δ_T (Figure A1). Suppose P-wave data acquired over such a model are migrated with the parameters $V_{P0,M}$, ϵ_M, and δ_M. Clearly, for a horizontal reflector the image point does not move laterally. Therefore, the reflection traveltimes in the true (t_T) and migration (t_M) models for the half-offset h can be written as

$$t_T = \frac{\sqrt{h^2+z_T^2}}{V_{g,T}(\phi)} \qquad \text{(A1)}$$

and

$$t_M = \frac{\sqrt{h^2+z_M^2}}{V_{g,M}(\phi')}, \qquad \text{(A2)}$$

where $V_{g,T}$ is the group velocity at the group angle ϕ in the true model, and $V_{g,M}$ is the group velocity at the group angle ϕ' in the model used for migration.

Under the assumption of weak anisotropy, quadratic and higher-order terms in the anisotropic coefficients can be neglected, and the group velocity can be replaced with the corresponding phase velocity (Thomsen, 1986; Tsvankin, 2001):

$$V_{g,T}(\phi) = V_{P0,T}\,[1+\delta_T \sin^2\phi + (\epsilon_T-\delta_T)\sin^4\phi]. \qquad \text{(A3)}$$

Likewise, for the migration model

$$V_{g,M}(\phi') = V_{P0,M}\,[1+\delta_M \sin^2\phi' + (\epsilon_M-\delta_M)\sin^4\phi']. \qquad \text{(A4)}$$

Substituting equations (A3) and (A4) into equations (A1) and (A2), equating the true and migration traveltimes ($t_T^2 = t_M^2$) and linearizing the resulting expression in the anisotropic coefficients yields

$$\begin{aligned}(h^2+z_T^2)\gamma^2[1-2\delta_T\sin^2\phi - 2(\epsilon_T-\delta_T)\sin^4\phi] \\ = (h^2+z_M^2)[1-2\delta_M\sin^2\phi - 2(\epsilon_M-\delta_M)\sin^4\phi'],\end{aligned} \qquad \text{(A5)}$$

where $\gamma \equiv V_{P0,M}/V_{P0,T}$.
Substituting

$$\sin^2\phi = \frac{h^2}{h^2+z_T^2} \quad \text{and} \quad \sin^2\phi' = \frac{h^2}{h^2+z_M^2} \qquad \text{(A6)}$$

into equation (A5) and solving for z_M, we obtain

$$\begin{aligned}z_M^2 \approx{}& \gamma^2 z_T^2 + h^2(2\delta_M - 1 + \gamma^2 - 2\delta\gamma^2) \\ &- \frac{2(\epsilon_T-\delta_T)h^4\gamma^2}{h^2+z_T^2} + \frac{2(\epsilon_M-\delta_M)h^4}{(h^2+z_T^2)\gamma^2}.\end{aligned} \qquad \text{(A7)}$$

The coefficient of h^2 can be represented as

$$(2\delta_M - 1 + \gamma^2 - 2\delta\gamma^2) \approx -V_{P0,M}^2\left(\frac{1}{V_{\mathrm{nmo},M}^2} - \frac{1}{V_{\mathrm{nmo},T}^2}\right), \qquad \text{(A8)}$$

where $V_{\mathrm{nmo}} = V_{P0}\sqrt{1+2\delta} \approx V_{P0}\,(1+\delta)$. Similarly, the coefficient multiplied with $[2h^4/(h^2+z_T^2)]$ takes the form

$$\gamma^2(\epsilon_T-\delta_T) + \frac{(\epsilon_M-\delta_M)}{\gamma^2} \approx \left(\eta_M\frac{V_{\mathrm{nmo},M}^2}{V_{\mathrm{nmo},T}^2} - \eta_T\frac{V_{\mathrm{nmo},T}^2}{V_{\mathrm{nmo},M}^2}\right), \qquad \text{(A9)}$$

where $\eta = (\epsilon-\delta)/(1+2\delta) \approx \epsilon-\delta$. Therefore, equation (A7) can be rewritten in terms of V_{nmo} and η as

$$\begin{aligned}z_M^2 \approx{}& \gamma^2 z_T^2 - h^2 V_{P0,M}^2\left(\frac{1}{V_{\mathrm{nmo},M}^2} - \frac{1}{V_{\mathrm{nmo},T}^2}\right) \\ &+ 2\frac{h^4}{h^2+z_T^2}\left(\eta_M\frac{V_{\mathrm{nmo},M}^2}{V_{\mathrm{nmo},T}^2} - \eta_T\frac{V_{\mathrm{nmo},T}^2}{V_{\mathrm{nmo},M}^2}\right).\end{aligned} \qquad \text{(A10)}$$

APPENDIX B: Image gather in a factorized $v(z)$ medium

Here, we extend the results of Appendix A to factorized $v(z)$ VTI media defined by the vertical velocity $V_{P0,T}$

at zero depth, the vertical velocity gradient $k_{z,T}$, and Thomsen parameters ϵ_T and δ_T. The one-way zero-offset time τ can be found as the following function of depth z:

$$\begin{aligned}\tau &= \int_0^z \frac{d\xi}{V(\xi)} \\ &= \int_0^z \frac{d\xi}{V_{P0,T} + k_{z_T}\,\xi} \\ &= \frac{1}{k_{z,T}} \ln\left[\frac{V_{P0,T} + k_{z,T}\,z}{V_{P0,T}}\right]. \end{aligned} \tag{B1}$$

Expressing z as a function of τ yields

$$z = \frac{V_{P0,T}}{k_{z,T}}(e^{k_{z,T}\,\tau} - 1)\,. \tag{B2}$$

Substituting z into the equation $V_{P0,T}(z) = V_{P0,T} + k_{z,T}\,z$ allows us to represent the vertical velocity as a function of the zero-offset time:

$$V_{P0}(\tau) = V_{P0,T}\,e^{k_{z,T}\,\tau}. \tag{B3}$$

Then the interval NMO $[V_{\rm nmo}(\tau)]$ velocity is given by

$$V_{\rm nmo}(\tau) = V_{P0,T}\,\sqrt{1+2\delta_T}\,e^{k_{z,T}\,\tau}. \tag{B4}$$

Applying the Dix formula and substituting equation (B4), we obtain the effective NMO velocity for a reflector at the depth z_T:

$$\begin{aligned} v^2_{{\rm nmo},T}(\tau_0) &= \frac{1}{\tau_0}\int_0^{\tau_0} V^2_{\rm nmo}(\tau)d\tau, \\ &= \frac{V^2_{P0,T}(1+2\delta_T)}{2\,\tau_0\,k_{z,T}}\left[e^{2k_{z,T}\,\tau_0} - 1\right], \text{ or} \\ v^2_{{\rm nmo},T}(t_0) &= \frac{V^2_{P0,T}(1+2\delta_T)}{t_0\,k_{z,T}}\left[e^{k_{z,T}\,t_0} - 1\right], \end{aligned} \tag{B5}$$

where $t_0 = 2\tau_0$ is the two-way time.

As shown in Appendix 4B of Tsvankin (2001), the zero-offset time t_0, the NMO velocity $v_{\rm nmo}$, and the parameter $\hat\eta$, which is defined as

$$\begin{aligned}\hat\eta_T &= \frac{1}{8}\left\{\frac{(1+8\eta_T)}{v^4_{{\rm nmo},T}(t_0)\,t_0}\left[\int_0^{t_0} V^4_{\rm nmo}(t)dt\right] - 1\right\} \\ &= \frac{1}{8}\left\{\frac{(1+8\eta_T)(e^{2k_{z,T}t_0}-1)k_{z,T}t_0}{2(e^{k_{z,T}\,t_0}-1)^2} - 1\right\}, \end{aligned} \tag{B6}$$

fully determine reflection moveout from horizontal interfaces in $v(z)$ VTI media. Hence, for the purpose of migrating horizontal events, the true factorized $v(z)$ medium can be replaced by a homogeneous VTI model with the vertical velocity equal to the average vertical velocity ($\hat V_{P0,T}$) above the reflector, the NMO velocity equal to $v_{{\rm nmo},T}$, and the parameter η equal to $\hat\eta_T$. Note that $\hat\eta_T$ depends on t_0, and hence, on the depth z_T. For a migrated image point at the half-offset h, the same substitutions can be used to replace the factorized $v(z)$ migration model above the image point with an equivalent homogeneous model. Therefore, the linearized equation of an image gather for a factorized $v(z)$ medium can be adapted from equation (A10) for homogeneous media:

$$\begin{aligned} z^2_M(h) &\approx z^2_M(0) \\ &- h^2\,\hat V^2_{P0,M}[z_M(h)]\left\{\frac{1}{v^2_{{\rm nmo},M}[z_M(h)]}\right. \\ &- \left.\frac{1}{v^2_{{\rm nmo},T}(z_T)}\right\} \\ &+ 2\frac{h^4}{h^2+z_T^2}\left\{\hat\eta_M\,\frac{v^2_{{\rm nmo},M}[z_M(h)]}{v^2_{{\rm nmo},T}(z_T)}\right. \\ &- \left.\hat\eta_T\,\frac{v^2_{{\rm nmo},T}(z_T)}{v^2_{{\rm nmo},M}[z_M(h)]}\right\}, \end{aligned} \tag{B7}$$

where $z_M(0) = \gamma z_T$, $\gamma = \hat V_{P0,M}/\hat V_{P0,T}$, $\hat V_{P0}$ is the average vertical velocity of the overburden, $\hat\eta_M \equiv \hat\eta[z_M(h)]$, $\hat\eta_T \equiv \hat\eta(z_T)$, and the NMO velocities are computed from equation (B5). When the migration model is close to the true model, $z_M(h) \approx z_M(0)$ for a moderate offset range. Then equation (B7) can be rewritten as

$$\begin{aligned} z^2_M(h) &\approx z^2_M(0) \\ &- h^2\hat V^2_{P0,M}\left\{\frac{1}{v^2_{{\rm nmo},M}[z_M(0)]} - \frac{1}{v^2_{{\rm nmo},T}(z_T)}\right\} \\ &+ 2\frac{h^4}{h^2+z_T^2}\left\{\hat\eta_M\,\frac{v^2_{{\rm nmo},M}[z_M(0)]}{v^2_{{\rm nmo},T}(z_T)}\right. \\ &- \left.\hat\eta_T\,\frac{v^2_{{\rm nmo},T}(z_T)}{v^2_{{\rm nmo},M}[z_M(0)]}\right\}. \end{aligned} \tag{B8}$$

Essentially, equation (B8) is based on the assumption that the effective quantities for the actual depth $z_M(h)$ can be replaced with those for $z_M(0)$. Note, however, that equation (B8) does not involve this approximation if the image gather is obtained after migration with a homogeneous VTI medium with the vertical velocity equal to $\hat V_{P0}[z(0)]$, NMO velocity equal to $v_{{\rm nmo},M}[z(0)]$, and $\hat\eta$ equal to $\hat\eta[z(0)]$.